Effect of Oily Additives on Foamability and Foam Stability. 2. Entry Barriers

Asen Hadjiiski,[†] Slavka Tcholakova,[†] Nikolai D. Denkov,*[,†] Patrick Durbut,[‡] Guy Broze,[‡] and Ammanuel Mehreteab[§]

Laboratory of Chemical Physics Engineering (Formerly Laboratory of Thermodynamics and Physicochemical Hydrodynamics), Faculty of Chemistry, Sofia University, 1 James Bourchier Avenue, 1164 Sofia, Bulgaria, Colgate-Palmolive Technology Center, 909 River Road, Piscataway, New Jersey 08854-5596, and Colgate-Palmolive Research & Development, Inc., Avenue Du Parc Industriel, B-4041 Milmort (Herstal), Belgium

Received April 24, 2001. In Final Form: July 23, 2001

In the preceding paper of this series we studied the effect of several oils of different chemical structure on the foaming properties of sodium dodecylbenzenesulfonate solutions. A straightforward correlation was found between the foam stability and the so-called "entry barrier", which prevents the emergence of pre-emulsified oil drops on the solution surface. In the present article we perform a systematic experimental study of the entry barriers for several oils by means of the recently developed film trapping technique. The latter consists of trapping oil drops in wetting films on a solid substrate, followed by a controlled increase of the capillary pressure of the meniscus that compresses the drops against the substrate. At a certain critical capillary pressure, P_C^{CR}, the asymmetric oil−water−air films rupture and the drops enter the water−air interface. This event is observed microscopically, and P_C^{CR} is determined as a function of various parameters (type of oil, surfactant concentration, drop size, and others). The entry barrier increases with the surfactant concentration, especially in the range where the surfactant micelles are expected to stabilize the asymmetric films. The results obtained with a series of alkanes (from octane to hexadecane) show that the entry barrier increases with the alkane chain length. Furthermore, it is shown that the presence of a spread oil (even as an ultrathin, molecular layer) on the surface of the foam film might lead to a significant change of the magnitude of the entry barrier. For decane and dodecane, the layer of spread oil reduces the entry barrier, whereas for hexadecane the effect is the opposite. As far as we know, such a role of oil spreading in the antifoaming action of oils has not been reported so far. Since the stability of thin liquid films is usually discussed in the literature in terms of the disjoining pressure, we estimate from the experimental data the critical disjoining pressure, Π_{AS}^{CR}, at which the asymmetric oil−water−air film ruptures and the drop entry occurs. The estimates show that the curvature of the asymmetric film is very important in the overall consideration of the mechanical equilibrium in the system and there is a big difference between the numerical values of P_C^{CR} and Π_{AS}^{CR}, unlike the case of planar films where $P_C^{CR} = \Pi_{AS}^{CR}$. Additionally, we find that P_C^{CR} is a weak function of the oil drop size and of the asymmetric film radius, while Π_{AS}^{CR} scales as (film radius)$^{-1}$ for all of the studied systems. These results are discussed with respect to the possible mechanisms of film rupture. Concerning the foam stability, P_C^{CR} is a more convenient quantity for description of the entry barriers, because its magnitude correlates with the foam height, whereas the magnitude of Π_{AS}^{CR} does not.

1. Introduction

In the first paper of this series[1] we studied how several oils of different chemical structure affected the foam stability and the foamability of sodium dodecylbenzenesulfonate (SDDBS) solutions. The results from the foam tests demonstrated a straightforward correlation between the foam stability and the entry barrier, which prevents the emergence of pre-emulsified oil drops on the solution surface (the used definition of the entry barrier is explained below). On the other hand, no direct relation between the foam stability and the magnitudes of the so-called entry, E, spreading, S, and bridging, B, coefficients was observed (most of the studied oils had positive B coefficients, which means that oil bridges, once formed in the foam films, would be unstable[2−4]).

Similar results were obtained recently with other surfactant−oil couples,[5−7] and a quantitative relation between the final foam height and the entry barrier was established.[5] The primary reason for this correlation is that any mechanism of foam destruction by emulsified oil should include the stage of formation and rupture of asymmetric oil−water−air films.[1,3,8−18] As noticed long ago by Kruglyakov[8] and Kulkarni et al.,[15] these asym-

* To whom correspondence may be addressed. Phone: (+359) 2-962 5310. Fax: (+359) 2-962 5643. E-mail: ND@LTPH.BOL.BG.

[†] Laboratory of Chemical Physics Engineering, Sofia University.

[‡] Colgate-Palmolive Research & Development, Inc., Milmort (Herstal).

[§] Colgate-Palmolive Technology Center, Piscataway.

(1) Arnaudov, L.; Denkov, N. D.; Surcheva, I.; Durbut P.; Broze G.; Mehreteab, A. *Langmuir* **2001**, *17*, 6999−7010.

(2) Garrett, P. R. *J. Colloid Interface Sci.* **1980**, *76*, 587.

(3) Garrett, P. R. In *Defoaming*: *Theory and Industrial Applications*; Garrett, P. R., Ed.; Marcel Dekker: New York, 1993; Surfactant Science Series, Vol. 45, Chapter 1.

(4) Denkov, N. D. *Langmuir* **1999**, *15*, 8530.

(5) Basheva E.; Ganchev, D.; Denkov, N. D.; Kasuga, K.; Satoh, N.; Tsujii, K. *Langmuir* **2000**, *16*, 1000. Basheva E.; Stoyanov, S.; Denkov, N. D.; Kasuga, K.; Satoh, N.; Tsujii, K. *Langmuir* **2001**, *17*, 969.

(6) Marinova, K.; Denkov, N. D. *Langmuir* **2001**, *17*, 2426.

(7) Denkov, N. D.; Marinova K. *Proceedings of the 3rd EuroConference on Foams, Emulsions and Applications*; MIT: Bremen, 2000.

(8) Kruglyakov, P. M.; Koretskaya, T. A. *Kolloid. Zh.* **1974**, *36*, 682. Kruglyakov, P. M. In *Thin Liquid Films: Fundamentals and Applications*; Surfactant Science Series; Ivanov, I. B., Ed.; Marcel Dekker: New York, 1988; Vol. 29, Chapter 11.

(9) Exerowa, D.; Kruglyakov, P. M. *Foams and Foam Films*; Elsevier: Amsterdam, 1998; Chapter 9.

(10) Bergeron, V.; Fagan, M. E.; Radke, C. J. *Langmuir* **1993**, *9*, 1704.

(11) Lobo, L.; Wasan, D. T. *Langmuir* **1993**, *9*, 1668.

10.1021/la010601j CCC: $20.00
Published on Web 09/29/2001

metric films might be stabilized by various surface forces (electrostatic, van der Waals, etc.), which suppress the drop entry and impede the antifoam action of oil. Furthermore, if the asymmetric film is stable, the introduction of oil into the foaming solution might lead to a foam-boosting effect (i.e., to more voluminous and stable foam) due to (i) reduced dynamic surface tension of the solutions[1,5] and (ii) decelerated water drainage, as a result of the Plateau border obstruction by oil drops.[13] Hence the oil drop entry is a key stage in the overall process of foam destruction by oils.

Several different parameters have been suggested in the literature to quantify the entry barriers for oil drops. Lobo and Wasan[11] suggested to use the energy of interaction per unit area in the asymmetric oil−water−air film, f, as a criterion of its stability

$$f = -\int_{h\to\infty}^{h_E} \Pi_{AS}\, dh \qquad (1)$$

where $\Pi_{AS}(h)$ is the disjoining pressure, while h_E is the equilibrium thickness of the asymmetric film at a certain capillary pressure (which has to be specified). In a parallel study, Bergeron et al.[10] suggested the so-called generalized entry coefficient

$$E_g = -\int_0^{\Pi_{AS}(h_E)} h\, d\Pi_{AS} \qquad (2)$$

where the lower limit of the integral corresponds to $\Pi_{AS}(h\to\infty) = 0$. As shown by Bergeron et al.,[10] the classical entry coefficient, E, can be obtained as a particular case of E_g in the limit $h_E \to 0$. One can deduce from eqs 1 and 2 that f and E_g are interrelated: $f(h_E) + E_g(h_E) = -h_E\, \Pi_{AS}(h_E)$.

The determination of the values of f and E_g and their comparison with the antifoam efficiency of different oils is a difficult task, because one needs to know the disjoining pressure isotherms, $\Pi_{AS}(h)$. The most thorough analysis of this type was carried out by Bergeron et al.[10] who measured the disjoining pressure isotherms of planar foam and asymmetric oil−water−air films for several surfactant−oil couples. They found a good correlation between the stability of the asymmetric films and the stability of foams in porous media, in the presence of oil. Furthermore, Bergeron et al.[10] showed that the destabilizing effect of oil is indeed caused by a lower stability of the asymmetric oil−water−air films as compared to the stability of the foam air−water−air film.

In the same study,[10] another possible quantity as a measure of the asymmetric film stability was also discussed, namely, the critical capillary pressure leading to rupture of the asymmetric film. A similar idea had been used before[19] to explain the collapse of foams in porous media in the absence of oil—as shown by Aronson et al.,[20] the measured value of the foam collapse pressure (which acts as to suck liquid from the foam) was close to the rupture pressure of a single foam film, as determined by the porous plate method.[21] Indeed, the critical capillary pressure seems to be the most adequate measure of the film stability in such systems, because the capillary pressure is the actual external variable that compresses the film surfaces toward each other, against the repulsive surface forces (disjoining pressure) stabilizing the film. The quoted authors studied *planar* films, where the imposed capillary pressure in equilibrium is exactly equal to the disjoining pressure;[10] that is, the concept of the critical *capillary pressure*, P_C^{CR}, is equivalent to the concept of the critical *disjoining pressure*, Π^{CR}. Bergeron[22] showed with foam films that, in some systems, the measured Π^{CR} corresponded to an actual maximum of the calculated DLVO-curve representing $\Pi(h)$, whereas Π^{CR} was well below the maximum of the calculated $\Pi(h)$ curves in other systems (for a possible explanation see Discussion in ref 22).

Recently, another experimental tool became available for quantifying the entry barriers of oil drops. Hadjiiski et al.[23−25] developed the so-called film trapping technique (FTT), which consists of trapping oil drops in a wetting film, formed from surfactant solution on a solid substrate, and a subsequent measurement of the critical capillary pressure that leads to drop entry on the fluid surface of the wetting film (see below for details). It is worthwhile noting several important features of the FTT: First, the FTT allows an independent variation of the radius of the asymmetric oil−water−air film and of the applied capillary pressure in a relatively wide ranges. Therefore, the dependence of P_C^{CR} and Π_{AS}^{CR} on the size of the asymmetric film can be investigated. The obtained results indicate a strong dependence of Π_{AS}^{CR} on the size of the asymmetric films (see below), which means that the critical pressures for microscopic and macroscopic films might be very different. Second, experiments with real antifoam drops of micrometer size can be carried out, giving a quantitative measure of the entry barrier that can be used to explain the foam stability.[5] Third, the asymmetric films formed in both the FTT and the real foams are strongly curved (radius of curvature on the order of micrometers), which means that the imposed capillary pressure is not equal to the disjoining pressure that stabilizes the film.[26] Hence an additional analysis is required to interpret the experimental data (measured in terms of P_C^{CR}) from the viewpoint of the surface forces stabilizing the asymmetric film (expressed by Π_{AS}). This analysis gives also information about the shape of the trapped drops, which are typically strongly deformed under the compressing force created by the water−air meniscus. Fourth, the method can be applied to different types of films (asymmetric oil−water−air, emulsion and foam films), so that a comparison of their stability for a given surfactant−oil system is possible. Last but not least, FTT requires relatively simple

(12) Koczo, K.; Koczone, J. K.; Wasan, D. T. *J. Colloid Interface Sci.* **1994**, *166*, 225.
(13) Koczo, K.; Lobo, L. A.; Wasan, D. T. *J. Colloid Interface Sci.* **1992**, *150*, 492.
(14) Wasan, D. T.; Christiano, S. P. In *Handbook of Surface and Colloid Chemistry*; Birdi, K. S., Ed.; CRC Press: Boca Raton FL, 1997; Chapter 6.
(15) Kulkarni, R. D.; Goddard, E. D.; Kanner, B. *J. Colloid Interface Sci.* **1977**, *59*, 468.
(16) Aveyard, R.; Binks, B. P.; Fletcher, P. D. I.; Peck, T. G.; Garrett, P. R. *J. Chem. Soc., Faraday Trans.* **1993**, *89*, 4313. Aveyard, R.; Binks, B. P.; Fletcher, P. D. I.; Peck, T. G.; Rutherford, C. E. *Adv. Colloid Interface Sci.* **1994**, *48*, 93.
(17) Bergeron, V.; Cooper, P.; Fischer, C.; Giermanska-Kahn, J.; Langevin, D.; Pouchelon, A. *Colloids Surf., A* **1997**, *122*, 103.
(18) Denkov, N. D.; Cooper, P.; Martin, J.-Y. *Langmuir* **1999**, *15*, 8514.
(19) Khatib, Z. I.; Hirasaki, G. J.; Falls, A. H. *SPE Reservoir Eng.* **1988**, *3*, 919.
(20) Aronson, A. S.; Bergeron, V.; Fagan, M. E.; Radke, C. J. *Colloids Surf., A* **1994**, *83*, 109.
(21) Mysels, K.; Jones, A. *J. Phys. Chem.* **1964**, *68*, 3441.
(22) Bergeron, V. *Langmuir* **1997**, *13*, 3474.
(23) Hadjiiski, A.; Dimova, R.; Denkov, N. D.; Ivanov, I. B.; Borwankar, R. *Langmuir* **1996**, *12*, 6665.
(24) Hadjiiski, A.; Tcholakova, S.; Ivanov, I. B.; Gurkov, T. D.; Leonard, E. *Langmuir*, in press.
(25) Hadjiiski, A.; Tcholakova, S.; Denkov, N. D.; Ivanov, I. B. *Proceedings of the 13th Symposium on Surfactants in Solution (SIS 2000)*; Gainsville, FL, June 2000; in press.
(26) Ivanov, I. B.; Kralchevsky, P. A. In *Thin Liquid Films*: *Fundamentals and Applications*; Surfactant Science Series; Ivanov, I. B., Ed.; Marcel Dekker: New York, 1988; Vol. 29, Chapter 2.

and cheap equipment, and after accumulating some experience one can rapidly obtain a large set of data. These features make the method an interesting complement and/or alternative to the classical porous plate method, from both fundamental and practical viewpoints.

In the present article we make a systematic experimental study of the entry barriers for several oils of different chemical structure by means of the FTT. Along with the practical question about the comparison of the entry barriers and their importance for the foam stability, we address also several other issues. The results prove that the presence of a spread oil (even as an ultrathin, molecular layer) on the surface of the foam film might lead to a significant change of the entry barrier. The critical disjoining pressure, Π_{AS}^{CR}, is estimated from the experimental data, and the curvature of the asymmetric films is found to be very important for the overall consideration of the mechanical equilibrium. It is shown that Π_{AS}^{CR} scales as (film radius)$^{-1}$ for all of the studied systems—an observation that calls for explanation and that poses a number of interesting questions concerning the mechanism of film rupture. Let us note here that the major aim of the present work is to clarify some of the factors affecting the entry barrier, rather than to understand and explain the mechanism of film rupture. The latter task requires additional experimental and theoretical efforts.

2. Experimental Details

2.1. Materials. Sodium dodecylbenzenesulfonate, SDDBS (product of Aldrich), is used as a main surfactant. The working solutions contain also 12 mM NaCl and 0.15 vol % of emulsified oil. The following oils are studied: *n*-octane, *n*-C_8; *n*-decane, *n*-C_{10}; *n*-dodecane, *n*-C_{12}; *n*-hexadecane, *n*-C_{16}; *n*-heptanol, *n*-C_7OH; *n*-dodecanol, *n*-$C_{12}OH$; 2-butyloctanol, 2BO; isohexyl-neopentanoate, IHNP; silicone oil SH200 of dynamic viscosity 5 mPa·s, SO. The *n*-alkanes are products of Sigma Co. Details about the other chemicals are given in ref 1. Hexadecane is refined by passing it through a glass column filled with chromatographic adsorbent (Florisil). The other chemicals are used as received. The solutions are prepared with deionized water from Milli-Q Organex system (Millipore). The oily additives are emulsified in the surfactant solutions by intensive stirring on a magnetic stirrer for 12 h.

2.2. Methods and Procedures. 2.2.1. Film Trapping Technique (FTT). The critical capillary pressure leading to rupture of the asymmetric oil—water—air film and to subsequent oil drop entry is measured by the FTT[24,25] (Figure 1). A vertical glass capillary, a few millimeters in radius, is positioned at a small distance above the flat bottom of a glass vessel. The lower end of the capillary is immersed in the working solution, which contains dispersed emulsion drops. The capillary is connected to a pressure control system, which allows one to vary and to measure the difference, ΔP_A, between the air pressure in the capillary, P_A, and the ambient atmospheric pressure, P_A^0. The data acquisition equipment includes a pressure transducer (Omega Engineering, Inc., Stamford, U.S.A.) and a digital multimeter Metex M-4660A (Metex Instruments) connected to a PC. The specifications of the used pressure sensors are presented in Table 1.

When P_A increases, the air—water meniscus in the capillary is pushed against the glass substrate and a wetting film is formed, which traps some of the oil drops (Figure 1B). These drops remain sandwiched between the air—water meniscus and the glass substrate. The capillary pressure of the air—water meniscus around the trapped drops is $P_C = P_A - P_W$, where P_W is the pressure in the liquid around the drops, which can be determined from the liquid level in the external part of the vessel (outside the capillary). The height of water there is $Z + Z_C$, where Z is the distance between the flat air—water interface and the lower capillary end, whereas Z_C is the distance between the substrate and the capillary end (Figure 1B). Thus the pressure at the bottom of the liquid is $P_A^0 + \rho_W g(Z + Z_C)$, where ρ_W is the water mass density and g is the acceleration of gravity. If one neglects the small variation of the hydrostatic pressure in the meniscus region inside the capillary ($Z_C \ll Z$), one finds the following relationship between the capillary pressure, P_C, and the measured pressure difference, ΔP_A

$$P_C = \Delta P_A - \rho_W g Z \qquad (3)$$

The depth of the liquid, Z, is measured during the submersion of the capillary in the solution (before starting the actual experiments) by a micrometer translator having an accuracy of ±5 μm, which corresponds to precision of ±0.05 Pa in the determination of the hydrostatic pressure (the last term in eq 3).

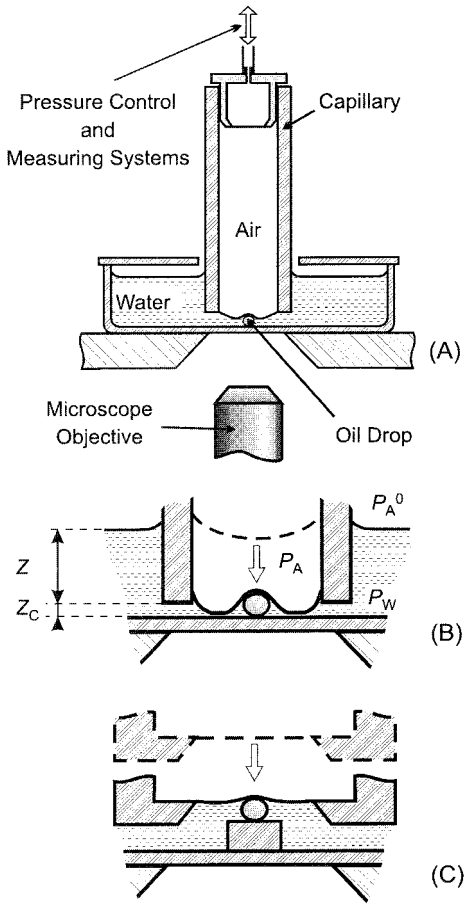

Figure 1. Scheme of the experimental setup and the basic principle of operation of the film trapping technique (FTT). (A) A vertical capillary, partially immersed in surfactant solution containing oil drops, is held close above the bottom of the experimental vessel. (B) The air pressure inside the capillary, P_A, is increased, and the water—air meniscus in the capillary is pressed against the glass substrate. Some of the oil drops remain trapped in the wetting glass—water—air film and are compressed by the meniscus. At a given critical capillary pressure (see section 2.2 for details) the asymmetric film formed between the oil drop and the solution surface ruptures and a drop entry event is observed by an optical microscope. (C) Another modification called "gentle FTT" is used for measuring very low entry barriers (below 20 Pa); a flat meniscus is formed, which allows the trapping of drops at virtually zero capillary pressure.

Table 1. Model and Main Characteristics of the Used Pressure Sensors

pressure transducer model[a]	pressure range, Pa	stated accuracy, Pa	stated hysteresis and repeatability, Pa
PX274-01DI	±125	<±1.25	±0.31
PX163-005BD5V	±1250	<±12.5	±3.1
PX142-001D5V	0—6900	<±51.8	±20.7

[a] Omega Engineering, Inc., Stamford, U.S.A.

During the experiment, one increases the pressure in the capillary, P_A, by very small increments. After each step of pressure increase, one waits for liquid drainage from the wetting film region and for reaching a mechanical equilibrium. The changes of the meniscus shape around the trapped drops (caused by the liquid drainage) are observed by optical microscope in reflected monochromatic light of wavelength $\lambda = 546$ nm; a characteristic interference pattern is seen, which changes with time if dynamic processes occur in the wetting film region. The equatorial diameter of the trapped drops, $2R_E$, is measured microscopically (in white transmitted light) with an accuracy of $\pm 0.8\ \mu$m. A Carl Zeiss Jena inverted microscope, equipped with objective LD Epiplan, 20×/0.40, digital CCD camera (Kappa CF 8/1 DX), and VCR (Panasonic NV−HD 680), is used for these observations.

The experiments show that the trapped drops enter (pierce) the surface of the wetting film at a given, critical capillary pressure, P_C^{CR}. The moment of drop entry, which is accompanied with a significant local change in the shape of the air−water interface, is clearly seen in both reflected and transmitted light. Therefore, the equipment allows one to measure P_C^{CR} as a function of the solution composition and drop radius. As mentioned above, for brevity we refer to P_C^{CR} as *the barrier to drop entry*. Larger P_C^{CR} corresponds to higher barriers (more difficult drop entry) and vice versa.

The experimental setup described above allows one to measure the entry barriers higher than ca. 20 Pa.[24] This limit is determined by the capillary pressure of the meniscus formed in the capillary before trapping the drops. Since the liquid wets the inner surface of the capillary, a spherical meniscus is formed of capillary pressure $P_C \approx 2\sigma_{AW}/R_{CAP} \sim 20$ Pa ($\sigma_{AW} \approx 30$ mN/m is the surface tension of the solution and $R_{CAP} \approx 3$ mm is the capillary radius). However, the barriers are sometimes lower and another modification of the method (called gentle FTT,[24,25] see Figure 1C) is used in such cases.

The main idea of the gentle FTT is to create a virtually flat air−water interface in the capillary before trapping the drops, so that P_C in the beginning of the experiment is almost zero. For this purpose, a sapphire disk of special design is attached to the lower end of the capillary. The disk has an opening with a wedgelike shape (Figure 1C), which ensures the stable attachment of the air−water interface to the sapphire upper edge. Additionally, a substrate with a small stub, cut out onto a glass plate, is used in these experiments. The plate is placed on the vessel's bottom, so that the stub is projected upward into the opening of the sapphire. One can move precisely the capillary in the $x-y-z$ directions and to juxtapose the flat fluid interface with the glass stub. Thus one can achieve trapping of drops by a flat interface, followed by a gentle increase of P_C until P_C^{CR} is reached.

2.2.2. Drop Entry Measurements in the Presence of Spread Oil Layer. One series of experiments is directed to reveal the effect of the oil layer, spread over the water−air interface, on the height of the drop entry barrier. For this purpose parallel experiments in the presence and in the absence of spread oil are performed.

For oils that are not very much soluble in the surfactant solution, like dodecane and hexadecane, a clean surface (free of spread oil) is created by pouring the studied emulsions into the experimental vessel for FTT experiments by the so-called "two-tips procedure" (TTP).[18] The latter consists of a gentle injection of the working emulsion through a narrow orifice (syringe needle or pipet tip)—in this way the oil layer, spread on the surface of the "mother" emulsion, is retained and a clean solution surface is created. It takes some period of time, which depends very much on the used oil and surfactant, before a new portion of spread oil appears due to coalescence of oil drops with the solution surface or to molecular transfer of oil.[18] Independent surface tension measurements reveal that the value of σ_{AW} of the dodecane and hexadecane emulsions, poured by the TTP, is virtually the same as that of the pure surfactant solution (without oil) and decreases very slowly with time—by less than 0.5 mN/m for a period of 1 h, which is about the time span of the typical FTT experiment. In these FTT tests, the number of the drop entry events observed in a single experiment is restricted to 6, to avoid the accumulation of detectable layer of spread oil from the entering drops.

The experiments, in which the effect of the spread layer is to be studied with water-soluble and volatile oils (octane, decane, 2BO, IHNP), are difficult and require a more complex procedure. When the oil drops are trapped in an wetting film, whose surface is cleaned from oil by the TTP, a significant oil evaporation through the asymmetric oil−water−air film occurs (evidenced by the rapid decrease of the drop size), because the air in the capillary is not saturated with oil vapors. The observed shrinking of the oil drops is certainly not caused by solubilization in the surfactant micelles, because the surfactant solutions are pre-equilibrated with oil and because no drop size reduction is observed before trapping the drops in the wetting film. Since the process of oil evaporation is very fast, the trapped oil drops disappear (evaporate) before the capillary pressure in the FTT equipment is increased up to the critical values, corresponding to drop entry. Hence it is impossible to measure the entry barrier with clean solution surface for these oils, because the air phase should be almost saturated with oil vapors to reduce the rate of oil evaporation, which inevitably leads to the formation of a spread oil layer.[27−29] That is why, we employed another procedure to study the effect of the spread layer on the entry barrier for the volatile oils. First, we measure the entry barrier for a solution surface saturated with oil, so that no drop evaporation takes place. In a separate experiment, which starts with saturated solution surface, we increase the capillary pressure up to a value just below the critical one. Afterward, maintaining the capillary pressure constant, we connect the air in the capillary with a much bigger volume of air ("buffer" of the same mechanical pressure), which is free from oil. As a result, the oil vapors diffuse into the buffer and the air in the capillary becomes undersaturated with oil. Thus an evaporation from the spread layer is induced, which is evidenced by the observed shrinking of the oil drops. In this moment, the capillary pressure is increased further, and a comparison of the entry barrier under these conditions (nonsaturated, evaporating oil layer) with the barrier in the presence of saturated oil layer becomes possible.

All experiments are carried out at the ambient room temperature ($T = 25 \pm 2$ °C). The experiments with n-$C_{12}OH$ are performed at 27 °C, to be well above its melting point (24 °C). The water evaporation inside the capillary is avoided, because the atmosphere above the wetting film is kept always saturated with aqueous vapors.

2.2.3. Surface Tension Measurements. The surface tension of the surfactant solution is measured by the Wilhelmy plate method, whereas the surface tension of the oil is measured by Du Nouy ring technique on Kruss K10T digital tensiometer. The interfacial tension of the oil−solution interface is measured by the pendant drop method.

3. Experimental Results and Discussion

3.1. Effect of SDDBS Concentration on the Drop Entry Barrier. 3.1.1. Critical Micelle Concentration (cmc) of SDDBS. The surface tension isotherm of the SDDBS in the presence of 12 mM NaCl shows no minimum around the cmc, which is an indication that the main surfactant is not contaminated by surface active impurities. The cmc obtained from the surface tension isotherm, 0.25 ± 0.1 mM, is in a reasonable agreement with the value 0.15 ± 0.05 mM measured by electrical conductivity (conductivity meter model 30, Denver Instrument Co., Arvada, CO). In the following discussions we use the mean value, cmc = 0.2 mM.

3.1.2. Dependence of P_C^{CR} on the Surfactant Concentration. This series of experiments is performed with drops of hexadecane, and the obtained results are shown in Figure 2. The working emulsion is poured in the experimental vessel by using the TTP to avoid the presence

(27) Aveyard, R.; Cooper, P.; Fletcher, P. D. I. *J. Chem. Soc., Faraday Trans.* **1990**, *86*, 3623.
(28) Aveyard, R.; Binks, B. P.; Fletcher, P. D. I.; MacNab, J. R. *Langmuir* **1995**, *11*, 2515.
(29) Binks, B. P.; Crichton, D.; Fletcher, P. D. I.; MacNab, J. R.; Li, Z. X.; Thomas, R. K.; Penfold, J. *Colloids Surf., A* **1999**, *146*, 299.

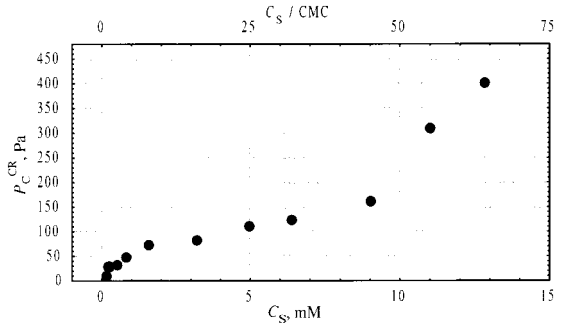

Figure 2. Dependence of the entry barrier, P_C^{CR}, on the SDDBS concentration, C_S, for hexadecane drops. All solutions contain 12 mM NaCl. The entry barriers are obtained with drops having approximately the same equatorial diameter $2R_E = 5.5 \pm 0.5$ μm. The solution surface is free from oil (the two-tips procedure is used to load the experimental cell). The size of the symbols corresponds to the accuracy of measurement.

of oil on the solution surface. The surfactant concentration, C_S, is varied between 0.16 and 12.8 mM (from 0.8 to 64 times cmc), while the salt concentration is fixed at 12 mM NaCl. To eliminate a possible effect of the drop size on the entry barrier, the average values obtained with drops of equatorial diameter, $2R_E$, confined between 5 and 6 μm are plotted in Figure 2. At least three independent experimental runs are carried out at a given value of C_S, with two to three entry events observed in each run. The reproducibility of the data is very good, typically ±5%.

The results shown in Figure 2 indicate a complex dependence of P_C^{CR} on the surfactant concentration: At concentrations below 0.16 mM (0.8 × cmc), the entry barrier is too low to be measured by the used experimental procedure. The main problem is that one observes numerous lenses of hexadecane covering the solution surface even after the TTP is used for loading the experimental cell − therefore, we could not prepare a solution surface free of oil for the entry experiments. At the lowest concentration where measurements are possible, $C_S = 0.16$ mM (0.8 × cmc), we obtained $P_C^{CR} = 10$ Pa. In the concentration range between 0.2 and 0.5 mM (1 to 2.5 × cmc), the entry barrier is almost constant, around 30 Pa. At higher concentrations, between 0.5 and 9 mM (2.5 to 45 × cmc), the barrier exhibits a slow but steady increase from ca. 40 to 150 Pa with the surfactant concentration. A much steeper increase of P_C^{CR} is observed at concentrations above 9 mM (45 × cmc) and the barrier is 400 Pa at $C_S = 12.8$ mM (64 × cmc).

The observed independence of the entry barrier on the surfactant concentration around the cmc can be explained by the facts that the surfactant adsorption layers are saturated in this concentration range and that there is no significant concentration of micelles in the solution. Therefore, all of the important characteristics determining the film stability, such as the surfactant adsorption, surface charge density, Debye screening length, Hamaker constant, etc., are virtually constant.

The observed sharp increase of P_C^{CR} at $C_S > 9$ mM is probably related to the stabilizing effect of the surfactant micelles trapped in the asymmetric oil−water−air film.[11,14,30−34] One can estimate that the effective volume fraction of the SDDBS micelles, Φ, including the contribution of the counterion atmosphere, is about 6% at the kink point (9 mM):

$$\Phi = \frac{4}{3}\pi R_\kappa^{\,3}\rho_M \qquad (4)$$

$$R_\kappa = \left(\frac{d_M}{2} + \kappa^{-1}\right)$$

ρ_M is the number concentration of micelles, $\kappa^{-1} = 2.6$ nm is the Debye screening length, and d_M is the actual diameter of the micelles (aggregation number $\nu_A = 50$ and $d_M = 5$ nm were adopted for this estimate). From the values of ρ_M and Φ, one can estimate the height of the last maximum (corresponding to one layer of micelles trapped in the film) in the oscillatory component of the disjoining pressure, by using the formulas from ref 30. The estimate shows that this maximum is about 73 Pa, which is not far away from the measured values of $P_C^{CR} \approx 160$ Pa (note that the electrostatic and van der Waals forces also contribute to the height of this maximum in the real film). Therefore, a detectable contribution of micelles in the stability of the films might be expected in this concentration range.

More difficult for explanation is the increase of P_C^{CR} in the intermediate concentration range, between 2.5 and 45 × cmc, because the micelles are not expected to play a significant role there. Most probably, the increase of P_C^{CR} is due to a gradual increase of the density of the surfactant adsorption layers on the oil−water and air−water interfaces. Indeed, the ionic strength of the ionic surfactant solutions increases above the cmc, due to the counterions dissociated from the micelles.[30,35] On the other side, the adsorption layers are denser at higher ionic strength, because the electrostatic repulsion between the ionized surfactant molecules is screened.[36] As a result, one may expect that the surfactant adsorption and the entry barrier increase above the cmc for ionic surfactants.

3.2. Drop Entry Barriers for Different Oils. All experiments described in sections 3.2 and 3.3 are carried out with solutions containing 2.6 mM SDDBS (≈13 × cmc) and 12 mM NaCl. The drop entry barriers for a series of *n*-alkanes (octane, decane, dodecane, hexadecane), 2BO, IHNP, heptanol, dodecanol, and silicone oil are measured. Drops of diameter between 2 and 12 μm are studied, and no significant dependence of P_C^{CR} on the drop size is observed. As a typical example, P_C^{CR} for dodecane drops is plotted in Figure 3 as a function of the equatorial drop diameter, $2R_E$. The points present the mean value of P_C^{CR} for drops of similar size, while the error bars show the standard deviation. Two curves are shown in Figure 3: The solid squares present the experimental data for 26 drops (5.0 ± 2.8 μm mean diameter) in the presence of a thin spread layer of oil on the solution surface. The empty squares present the experimental data for 27 drops (7.6 ± 2.8 μm mean diameter) in the absence of a spread oil−the working emulsions are poured by the TTP in these experiments. The barrier measured in the experiments with the spread oil layer is 48 ± 5 Pa, which is two times lower than the barrier for the surface free of oil (96 ± 5 Pa). Such a systematic change of the entry barrier in the presence of spread oil is detected with other systems as well and will be discussed in more detail in the next subsection. All experiments discussed hereafter in this section are performed with spread oil layer on the solution surface.

(30) Kralchevsky, P. A.; Denkov, N. D. *Chem. Phys. Lett.* **1995**, *240*, 385.
(31) Nikolov, A. D.; Wasan, D. T.; Kralchevsky, P. A.; Ivanov, I. B. *J. Colloid Interface Sci.* **1989**, *133*, 1, 13.
(32) Bergeron, V.; Radke, C. J. *Langmuir* **1992**, *8*, 3020.
(33) Pollard, M. L.; Radke, C. J. *J. Chem. Phys.* **1994**, *101*, 6979.
(34) Chu, X. L.; Nikolov, A. D.; Wasan, D. T. *Langmuir* **1994**, *10*, 4403.
(35) Richetti, P.; Kekicheff, P. *Phys. Rev. Lett.* **1992**, *68*, 1951.
(36) Davies, J.; Rideal, E. *Interfacial Phenomena*; Academic Press: New York, 1963.

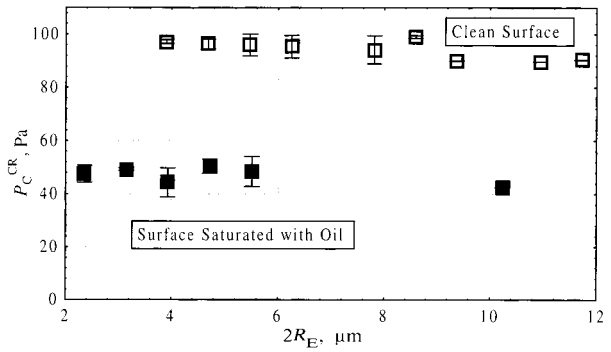

Figure 3. Drop entry barrier, P_C^{CR}, as a function of equatorial drop diameter, $2R_E$, measured for dodecane drops in aqueous solution of 2.6 mM SDDBS and 12 mM NaCl. The empty squares present the data for clean air−water surface (without a spread oil layer), whereas the solid squares present the data for solution surface, which is saturated with oil. The points present the mean values and the error bars are the standard deviation for drops of similar size.

Table 2. Drop Entry Barriers, P_C^{CR}, Measured for Different Oils with Solution Surface Saturated with Oil (the results shown in parentheses correspond to solution surface free of spread oil)[a]

oil	P_C^{CR}, Pa	V_F/V_{IN}
octane	30 ± 2	
decane	35 ± 5 (>70)	
dodecane	48 ± 5 (96 ± 5)	
hexadecane	400 ± 10 (80 ± 5)	0.94
2BO	44 ± 2	0.21
IHNP	75 ± 7	0.22
dodecanol	>1500	0.93
SO	>3000	0.86

[a] The aqueous solution contains 2.6 mM SDDBS and 12 mM NaCl. The ratio of the final over initial foam volumes, V_F/V_{IN} (as measured by the Ross−Miles method in ref 1), is also shown for comparison.

The mean values of the drop entry barrier, P_C^{CR}, measured for the different oils are summarized in Table 2. The results demonstrate that the entry barrier for *n*-alkane drops increases with the molecular mass of the alkane: for octane $P_C^{CR} = 30 \pm 2$ Pa, for decane $P_C^{CR} = 35 \pm 5$ Pa, for dodecane $P_C^{CR} = 48 \pm 5$ Pa, and for hexadecane $P_C^{CR} = 400 \pm 10$ Pa. The latter value is much higher than the value reported in the previous section, $P_C^{CR} = 80 \pm 5$ Pa, in the absence of a spread hexadecane layer (for discussion see section 3.3). Such a significant increase of the entry barrier with the alkane chain length is certainly important for the antifoam action of these oils, and systematic foam tests are planned soon to check quantitatively this relation.

The mean entry barrier for IHNP drops (Figure 4) is $P_C^{CR} = 75 \pm 7$ Pa, obtained as an average from 195 drops of diameter 6.6 ± 3.2 μm. For 2BO the barrier $P_C^{CR} = 44 \pm 2$ Pa (in this case 8 drops of diameter 6.4 ± 3.7 μm are observed). The experiments with drops of *n*-dodecanol with saturated surface reveal that the entry barrier is rather high—above 1500 Pa. Similarly, a very high entry barrier is measured with silicone oil (P_C^{CR} > 3 000 Pa). Note that these values correlate rather well with the results from the foam stability tests reported in ref 1.

It is worthwhile noting that no detectable drop shrinking (due to oil evaporation across the oil−water−air film) is observed with IHNP, 2BO, and hexadecane, when the studied emulsions are poured in the FTT equipment without using the TTP. This means that the surface of the surfactant solutions has been covered by a thin layer of oil (in the cases of 2BO and hexadecane, this layer is in

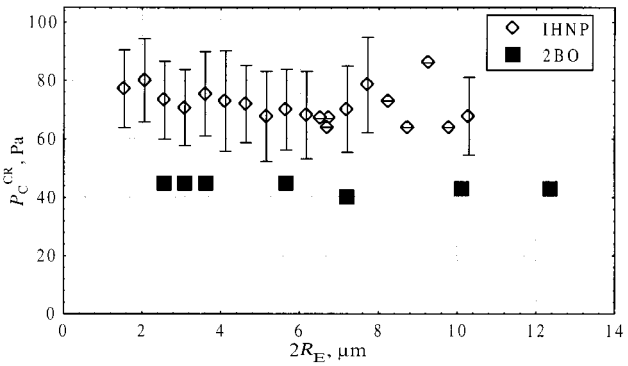

Figure 4. Drop entry barrier, P_C^{CR}, as a function of equatorial drop diameter, $2R_E$, measured for drops of IHNP (open diamonds) and 2BO (solid squares) in aqueous solution of 2.6 mM SDDBS and 12 mM NaCl.

equilibrium with oil lenses), which saturates the atmosphere with oil vapors, so that the evaporation from the drops is suppressed. This observation suggests that, probably, the oil evaporation was not a very important factor for the stability of the foams studied in ref 1, because the surface of the foaming solutions was always covered by an oil layer (this is evidenced by the reduced equilibrium and dynamic surface tension of these solutions—see Table 1 and Figure 4 in ref 1). However, we could not rule out the possibility that the foam destabilization in the presence of volatile oils, under certain conditions (e.g., when the foam is generated in open containers), could be affected by oil evaporation and the ensuing Marangoni effect, or other processes related to the oil volatility and solubility in the solutions (see also the comments at the end of section 4.2 below).

Results with heptanol are not shown in Table 2, because the wetting film around the trapped drops ruptures at $P_C \approx 60$ Pa. This event makes impossible the further increase of the capillary pressure of the meniscus compressing the drops; isolated water "islands" are formed around the heptanol drops, and there is no direct aqueous connection between these islands and the meniscus formed at the periphery of the wetting film.

The question about the actual reasons for the different entry barriers of the studied oils is very important, but the information available so far is rather insufficient to answer it. That is why we restrict our comment only to the list (probably nonexhaustive) of different factors that could affect significantly the entry barriers: (1) the density and the other properties of the surfactant adsorption layers on the oil−water interface;[8] (2) the formation of mixed oil−surfactant and/or of spread oil layers at the water−air interface;[27−29] (3) change of the micellar aggregation number due to oil solubilization;[37] (4) change in the micelle−micelle and micelle−surface interactions in the presence of solubilized oil.[38] All of these factors are rather specific for the different oils, and further systematic studies are needed to reveal their importance for the studied phenomenon.

3.3. Effect of the Spread Oil Layer on the Entry Barrier. As mentioned in section 3.2, the experiments with dodecane demonstrate a significant effect of the spread oil layer on the entry barrier of the drops—it is two times lower in the presence of spread dodecane. A similar effect of the spread oil was measured also for decane; the

(37) Nakagawa, T.; Shinoda, K. In *Colloidal Surfactants*; Shinoda, K., Nakagawa, T., Tamamushi, B., Isemura, T., Eds.; Academic Press: Orlando, FL, 1963; p 139.

(38) Lobo, L. A.; Nikolov, A. D.; Wasan, D. T. *J. Dispersion Sci. Technol.* **1989**, *10*, 143.

barrier obtained in the presence of spread layer was 35 ± 5 Pa, whereas the capillary pressure can be increased up to 70 Pa without drop entry to take place for a solution surface that is free of oil (the trapped drops evaporated without entry, as explained in section 2.2.2). Therefore the barrier for decane with a clean surface is at least two times higher than the barrier for the surface covered by a spread layer. On the contrary, the formation of a mixed adsorption layer SDDBS−hexadecane led to about a five times higher barrier (section 3.2) as compared to the barrier measured with solution surface free of hexadecane (section 3.1). Therefore, the presence of oils on the solution surface might significantly affect the magnitude of the entry barriers. It is rather possible that the high entry barrier observed with n-$C_{12}OH$ is similalry due to the formation of a dense mixed adsorption layer on the solution surface.[39,40]

The observed increase of the entry barrier with the molecular mass of the alkanes (from octane to hexadecane) might be also related to the structure of the formed spread or mixed layers on the solution surface. As shown by Aveyard, Binks and co-workers,[27−29] mixed adsorption layers are formed typically by long-chain alkanes ($>C_{11}$), which do not spread in the form of a multimolecular layer on the surface. On the contrary, the short-chain alkanes often either form a thin multimolecular layer or spread as a thick (duplex) film. It is worthwhile noting that the interaction of an oil drop with a solution surface covered by a thick oil layer would resemble the interaction of the drop with its own homophase (i.e., an oil−water−oil film of emulsion type will be formed), but a systematic comparison of the stability of the asymmetric oil−water−air and the emulsion oil−water−oil films is still missing.

Let us note at the end of this section that the observed change of the entry barrier in the presence of spread oil has an important implication for the antifoaming action of the oils. However, as discussed in refs 1, 3, 5, 6, 41, and many others, different factors are often more important and no straightforward correlation between the spreading behavior and the antifoam activity is observed.

4. Dependence of the Critical Disjoining Pressure for Film Rupture on the Film Size

The results presented in Figures 3 and 4 show that the critical *capillary* pressure, P_C^{CR}, is a very weak function of the size of the asymmetrical oil−water−air film. Additional analysis is needed, however, to understand how the critical *disjoining* pressure, Π_{AS}^{CR}, depends on the film size. In this section we investigate this dependence and discuss it from the viewpoint of the mechanism of rupture of the thin asymmetric films.

4.1. Estimation of the Critical Disjoining Pressure for Curved Asymmetric Films. 4.1.1. Disjoining Pressure for Spherical Films. The disjoining pressure, Π_{AS}, accounts for the interactions between the two film surfaces (van der Waals, elctrostatic, steric, etc.) and is conventionally defined as the surface force per unit area (a more general and rigorous definition was given through the components of the pressure tensor).[42,43] Positive

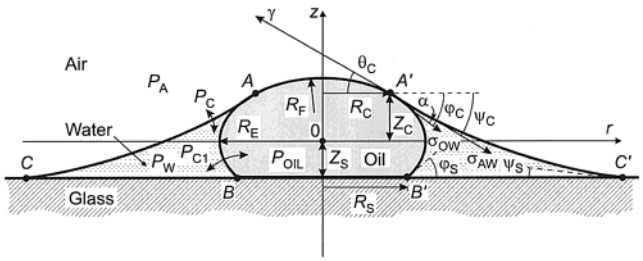

Figure 5. Schematic cross section of an oil drop trapped by water−air meniscus on a solid substrate. The arc AA' corresponds to the asymmetric (pseudoemulsion) oil−water−air film. The line BB' corresponds to the oil−water−glass film. The curves AC and $A'C'$ represent the air−water interface around the droplet. $P_C = (P_A - P_W)$ and $P_{C1} = (P_{OIL} - P_W)$ are the capillary pressures across the water−air and the oil−water interfaces, respectively.

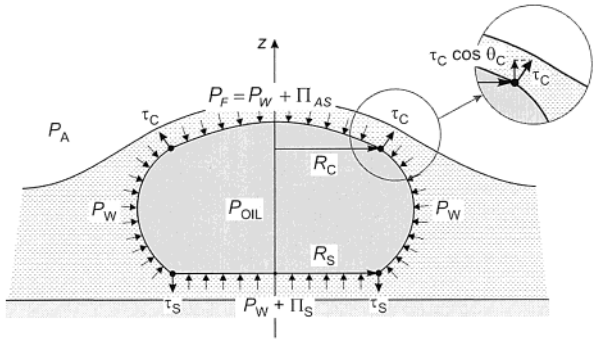

Figure 6. Schematic presentation of the forces (disjoining pressures and transversal line tensions), contributing to the vertically resolved balance of forces acting on the drop surface, eq 14.

disjoining pressure corresponds to a repulsive surface force (i.e., to film stabilization) and vice versa. In the case of planar films, the condition for mechanical equilibrium requires that the capillary sucking pressure must be exactly counterbalanced by the disjoining pressure.[42−45] However, the thin films in our experiments are curved and the condition for mechanical equilibrium is more complex, because it includes the capillary pressure jumps across the curved film surfaces. The relevant theoretical approach to this configuration was developed by Ivanov and Kralchevsky,[24,26,44] who showed that the disjoining pressure is related to the capillary pressure across the water−air interface, $P_C = P_A - P_W$, by the expression

$$\Pi_{AS} = P_F - P_W = (P_F - P_A) + (P_A - P_W) = \frac{2\sigma_{AW}}{R_F} + P_C \quad (5)$$

where P_F is the pressure in the asymmetric oil−water−air film and R_F is its radius of curvature (Figures 5 and 6). The aqueous phase, from which the asymmetric film is formed, is chosen as a referent phase for the definition of the disjoining pressure as usual.[26,44]

For micrometer-sized drops, R_F is on the order of the drop size and $2\sigma_{AW}/R_F > 10^4$ Pa. In most of our systems $P_C \approx 10^2$ Pa and can be neglected in eq 5. Thus only the radius of film curvature, R_F, would be sufficient to calculate Π_{AS}, because σ_{AW} is a known quantity (the slight change

(39) Lu, J. R.; Purcell, I. P.; Lee, E. M.; Simister, E. A.; Thomas, R. K.; Rennie, A. R.; Penfold, J. *J. Colloid Interface Sci.* **1995**, *174*, 441.
(40) Angarska, J. K.; Tachev, K. D.; Kralchevsky, P. A.; Mehreteab, A.; Broze G. *J. Colloid Interface Sci.* **1998**, *200*, 31.
(41) Garrett, P. R.; Davis, J.; Rendall, H. M. *Colloids Surf., A* **1994**, *85*, 159.
(42) Derjaguin, B. V. *Theory of Stability of Colloids and Thin Liquid Films*; Plenum, Consultants Bureau: New York, 1989.
(43) Ivanov, I. B., Ed. *Thin Liquid Films*: *Fundamentals and Applications*; Surfactant Science Series; Marcel Dekker: New York, 1988; Vol. 29.
(44) Kralchevsky, P. A. Effect of Film Curvature on the Thermodynamic Properties of Thin Liquid Films. Ph.D. Thesis, Sofia University, Sofia, Bulgaria, 1984 (in Bulgarian).
(45) Ivanov, I. B.; Toshev, B. V. *Colloid Polym. Sci.* **1975**, *253*, 558 and 593.

of the surface tension of the film due to the surface forces is neglected in eq 5, because it is a higher order effect). Note, however, that R_F depends on the drop deformation, which in turn is determined by the applied capillary pressure, P_C. For large drops or bubbles, one can measure directly the radius of film curvature, R_F, by using the microscopic method of differential interferometry,[46] but this method cannot be used for small, micrometer sized drops. That is why we apply below an indirect method to estimate the magnitude of Π_{AS} from the accessible experimental data and to study how the critical disjoining pressure for drop entry, Π_{AS}^{CR}, depends on the size of the asymmetric film.

4.1.2. Main Assumption. From the experiment we know the capillary pressure P_C, the equatorial drop radius R_E, and the interfacial tensions, σ_{AW} and σ_{OW}. To make the problem tractable and to estimate Π_{AS}, we make the assumption that the contact angles between the films and the adjacent menisci (see Figure 5) are known and have some small (fictitious) values: φ_S, angle of the oil−water−glass film; ψ_S, angle of the wetting glass−water−air film; α, angle of the curved asymmetric film. Since these angles are of the type liquid film−meniscus, they are typically below 5°. The numerical calculations revealed that the estimated disjoining pressure, Π_{AS}, is virtually insensitive to the chosen values of the contact angles in the range 0−5°. Therefore, for clarifying the effect of the film size on the value of Π_{AS}^{CR}, one may choose any value between 0 and 5° for these angles. Once the angles are chosen, one can calculate Π_{AS} from the experimental data as explained below. In most computations, we will use for simplicity $\varphi_S = \psi_S = \alpha = 0$. The influence of this assumption on the calculated values of Π_{AS} is checked a posteriori (see below).

4.1.3. Derivation of the Basic Equations. The shapes of the water−air and oil−water interfaces are described by solutions of the Laplace equation of capillarity, which can be presented in the following form for axially symmetric system:[47,48]

$$\frac{1}{r}\frac{d}{dr}(r \sin \phi_i) = 2k_i, \qquad k_i = \frac{P_{Ci}}{2\sigma_i} \tag{6}$$

$$\frac{dz}{dr} = \pm\tan \phi_i = \pm \frac{\sin \phi_i}{(1 - \sin^2 \phi_i)^{1/2}} \tag{7}$$

Here ϕ is the running slope angle of the interface and P_C is the capillary pressure. The index i denotes the following interfaces: $i = 1$ for the oil−water interface, $P_{C1} \equiv P_{OIL} - P_W$, $\sigma_1 \equiv \sigma_{OW}$; $i = 2$ for the air−water interface, $P_{C2} \equiv P_C = P_A - P_W$, $\sigma_2 \equiv \sigma_{AW}$.

Let us consider the shape of the drop interface described by eqs 6 and 7 for $i = 1$. The integration of eq 6 from the equatorial radius R_E to a given value of the running coordinate r leads to

$$\sin \phi_1(r) = \frac{1}{r}[k_1(r^2 - R_E^2) + R_E] \tag{8}$$

Substituting $\phi_1(R_S) = \varphi_S$ in eq 8, one derives an expression for the contact radius, R_S, of the drop with the substrate

$$R_S = \frac{\sin \varphi_S + (\sin^2 \varphi_S - 4k_1R_E(1 - k_1R_E))^{1/2}}{2k_1} \tag{9}$$

$$k_1R_E > 1$$

Similarly, one can express the angle φ_C, which is complementary to the slope angle of the drop generatrix at the contact line of the asymmetric film, $\phi_1(R_C)$

$$\varphi_C = \pi - \phi_1(R_C) = \arcsin\left[\frac{k_1}{R_C}(R_C^2 - R_E^2) + \frac{R_E}{R_C}\right] \tag{10}$$

The angles ψ_C and θ_C (Figure 5) can be expressed through φ_C in the following way

$$\psi_C = \varphi_C - \alpha \tag{11}$$

$$\theta_C = \arctan\left(\frac{\sigma_{AW} \sin \psi_C + \sigma_{OW} \sin \varphi_C}{\sigma_{AW} \cos \psi_C + \sigma_{OW} \cos \varphi_C}\right) \tag{12}$$

The last equation is a corollary of the horizontal and vertical balances of the interfacial tensions acting on the contact line[26,49] of the asymmetric film, with neglected effect of the line tension[50]

$$\sigma_{AW} \cos \psi_C + \sigma_{OW} \cos \varphi_C = \gamma \cos \theta_C$$

$$\sigma_{AW} \sin \psi_C + \sigma_{OW} \sin \varphi_C = \gamma \sin \theta_C$$

Here γ is the membrane tension[26] of the asymmetric film. From the geometric relation

$$R_F = R_C/\sin \theta_C \tag{13}$$

one obtains the radius of the film curvature, R_F. Therefore, if one knows the capillary pressure at the oil−water interface, P_{C1}, and the contact radius, R_C (which are still unknown at that stage), the disjoining pressure, Π_{AS}, can be calculated by means of eqs 5, 12, and 13.

An equation for calculating R_C can be derived from the *balance of the vertically resolved forces* acting on the trapped drop (the horizontal force balance is trivial, because the system is axially symmetric). Since the drop size is very small, one can neglect the variations of the hydrostatic pressure around the drop surface and assume that P_W is constant. Therefore, P_W does not contribute to the vertical force balance. The drop contacts with the substrate through the oil−water−glass film and with the air phase through the asymmetric oil−water−air film (see Figure 6). The condition for mechanical equilibrium in these two thin films implies that the respective disjoining pressures, arising from the interaction between the film surfaces, are exerted on the surface of the drop. Therefore, the vertical force balance includes the contributions of the disjoining pressures acting in the oil−water−air film, Π_{AS}, and in the film formed between the drop and the substrate, Π_S (multiplied by the respective projected film areas). Since the aqueous film between the drop and the substrate is planar, Π_S must be equal to the capillary pressure P_{C1}.

Along with the contribution of the disjoining pressures, the force balance includes the contributions of the linear

(46) Nikolov, A. D.; Kralchevsky, P. A.; Ivanov, I. B. J. *Colloid Interface Sci.* **1986**, *112*, 122.

(47) Kralchevsky, P. A.; Danov, K. D.; Denkov, N. D. In *Handbook of Surface and Colloid Chemistry*; Birdi, K. S., Ed.; CRC Press: New York, 1997; Chapter 11.

(48) Princen, H. M. In *Surface and Colloid Science*; Matijevic, E., Ed.; Wiley-Interscience: New York, 1969; Vol. 2, p 1.

(49) Kralchevsky, P. A.; Danov, K. D.; Ivanov, I. B. In *Foams*: *Theory, Measurements, and Applications*; Prud'homme, R. K., Khan, S. A., Eds.; Marcel Dekker: New York, 1995; Chapter 1.

(50) Ivanov, I. B.; Kralchevsky, P. A.; Nikolov, A. D. *J. Colloid Interface Sci.* **1986**, *112*, 97. Ivanov, I. B.; Kralchevsky, P. A.; Dimitrov, A. S.; Nikolov, A. D. *Adv. Colloid Interface Sci.* **1992**, *39*, 77.

forces acting on the contact lines of the films, due to so-called "transversal line tensions".[26,47] The vertical projection of the force created by the transversal tension at the contact line of the oil−water−air film is $2\pi R_C\tau_C \cos\theta_C$, where τ_C is the corresponding transversal tension

$$\tau_C = \sigma_{OW} \sin(\varphi_C - \theta_C)$$

The linear excess force acting on the contact line of the film with the glass substrate is $2\pi R_S\tau_S$, where τ_S is

$$\tau_S = \sigma_{OW} \sin \varphi_S$$

Thus one obtains the following balance of forces acting on the drop surface

$$\pi R_C{}^2\Pi_{AS} - 2\pi R_C\sigma_{OW} \cos\theta_C \sin(\varphi_C - \theta_C) = \pi R_S{}^2 P_{C1} - 2\pi R_S\sigma_{OW} \sin\varphi_S \quad (14)$$

The left-hand side of eq 14 presents the force acting in the region of the asymmetric oil−water−air film: the first term accounts for the disjoining pressure in the film, while the second term accounts for the transversal tension acting on the contact line. The right-hand side of eq 14 presents the corresponding terms for the film intervening between the drop and the substrate.

Finally, we should define a procedure for determination of the capillary pressure at the oil−water interface, P_{C1}. The procedure is based on the necessary geometrical *condition for matching the generatrix of the air−water meniscus* with the drop surface and with the substrate at the specified contact angles, ψ_C and ψ_S. The shape of the water−air meniscus can be obtained by integration of eqs 6 an 7 ($i = 2$, P_C is known from the experiment) with boundary conditions at the contact line of the asymmetric film

$$\phi_2(r) = -\psi_C; \quad r = R_C, \quad z = Z_C \quad (15)$$

This meniscus has to intersect the plane of the substrate at the following angle

$$\phi_2(r) = -\psi_S; \quad r = R_S, \quad z = -Z_S \quad (16)$$

Explicit expressions for $Z_C = z(R_C)$ and $Z_S = z(R_S)$ can be found from the solutions of the Laplace equation of capillarity (eq 6 and 7) for the drop surface ($i = 1$)[44,47]

$$z(r) = \pm\left[\left(R_E - \frac{1}{k_1}\right)F(\Lambda,q) - R_E\,E(\Lambda,q)\right] \quad (17)$$

$$R_1 \le r \le R_E, \quad k_1R_E > 1$$

where R_1, q, and $\Lambda(r)$ are defined as

$$R_1 = \left|\frac{1 - k_1R_E}{k_1}\right| \quad (18)$$

$$q = \left(1 - \frac{R_1{}^2}{R_E{}^2}\right)^{1/2}$$

$$\sin\Lambda = q^{-1}\left(1 - \frac{r^2}{R_E{}^2}\right)^{1/2}$$

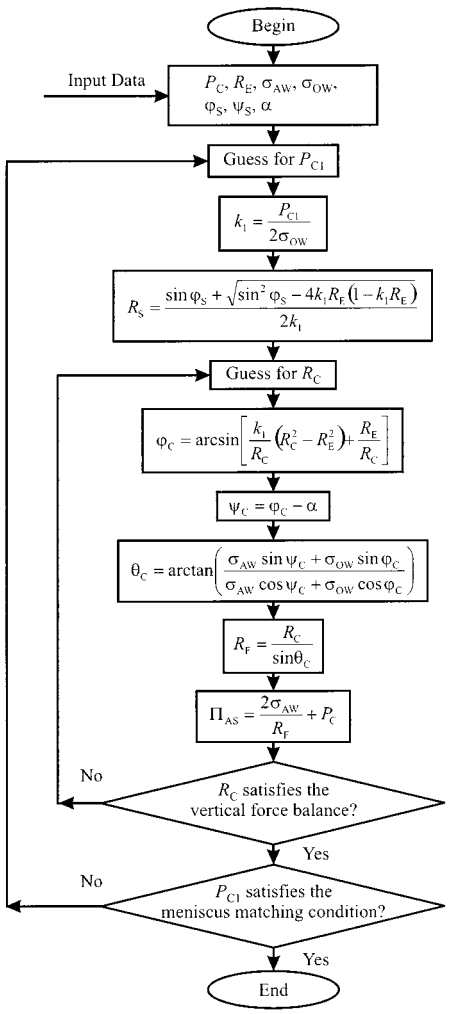

Figure 7. A block scheme of the iterative procedure for calculating the disjoining pressure, Π_{AS}, of the asymmetrical oil−water−air film (see section 4.1.4).

$F(\Lambda,q)$ and $E(\Lambda,q)$ are elliptic integrals of the first and second kind, respectively[51]

$$F(\Lambda,q) = \int_0^\Lambda \frac{d\xi}{(1 - q^2\sin^2\xi)^{1/2}} \quad (19)$$

$$E(\Lambda,q) = \int_0^\Lambda (1 - q^2\sin^2\xi)^{1/2}\,d\xi \quad (20)$$

Note that k_1 depends on P_{C1} (eq 6), which allows one to use eqs 15−17 for determination of P_{C1} (see the following subsection).

4.1.4. Numerical Iterative Procedure for Calculation of Π_{AS}. On the basis of the above analysis, one can calculate the disjoining pressure of the asymmetric film, Π_{AS}, by means of an iterative procedure whose block scheme is shown in Figure 7. One starts with an initial guess for the two independent unknowns—the capillary pressure of the drop, P_{C1}, and the contact radius of the asymmetric film, R_C (see Figure 5). From eq 9 one calculates a value for the contact radius drop substrate, R_S. Then, from eqs 10−12 one calculates the angles φ_C, ψ_C, and θ_C and by eqs 13 and 5, the radius of film curvature, R_F, and the disjoining pressure, Π_{AS}, respectively. One

(51) Abramowitz, M.; Stegun, I. A. *Handbook of Mathematical Functions*; Applied Mathematics Series; National Bureau of Standards, Washington, 1964; Vol. 55, Chapter 17 (reprinted by Dover Publications: New York, 1968).

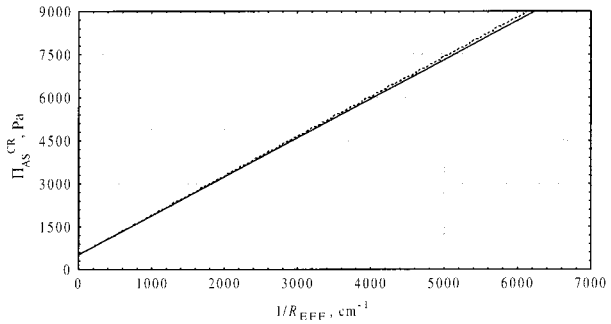

Figure 8. Dependence of the critical disjoining pressure, Π_{AS}^{CR}, on the inverse radius of the asymmetric film, $R_{EFF}^{-1} = (\pi A_F)^{-1/2}$; A_F is the actual area of the asymmetric film (corresponding to the arc AA′ in Figure 5). The calculations are made for 3.2 mM SDDBS, 12 mM NaCl, and hexadecane drops (clean water−air surface). The solid line represents the calculations with $\alpha = \varphi_S = 0°$, whereas the dashed line corresponds to $\alpha = \varphi_S = 5°$. The angle of the wetting glass−water−air film in both cases is $\psi_S = 0$ since direct microscope observations show that in all experiments this angle is virtually zero.

varies the value of R_C (and the corresponding values of φ_C, ψ_C, θ_C, R_F, and Π_{AS}) until the vertical force balance, eq 14, is satisfied. In another (larger) loop, one varies P_{C1} to satisfy the condition for matching the generatrix of the air−water meniscus at the contact lines with the drop and the substrate given by eqs 15 and 16. The variation of P_{C1} and R_C is performed by the minimization method of Brent.[52] The integration of the Laplace equation for the air−water meniscus, which is necessary for matching the interfaces, is performed by a fifth order Runge−Kutta method with adaptive step size control.[52] The procedure is implemented in a computer program written in C++ (Borland C++ Builder) with interactive user interface under Windows NT/98. The reliability of the calculations performed by this procedure is evidenced by experiments with larger drops (diameter above 100 μm), where a direct optical measurement of the radii R_C, R_S, and the contact radius of the air−water meniscus with the substrate is possible. These experiments reveal a very good agreement between the calculated and the measured values of the contact radii within the framework of experimental accuracy.

4.2. Numerical Results. In Figure 8, the calculated dependence of Π_{AS}^{CR} as a function of the inverse film radius for 3.2 mM SDDBS, 12 mM NaCl, and hexadecane drops (clean water−air surface) is shown by a solid line. The contact angles are taken as equal to zero, $\varphi_S = \psi_S = \alpha = 0$. Since the asymmetric film is curved, there are different possible definitions of its size. For this plot we have chosen the "effective" film radius to be equal to the radius of a planar film, which has the same area as the real asymmetric film

$$R_{EFF} = (A_F/\pi)^{1/2} \qquad (21)$$

where A_F is the actual area of the asymmetric film. As seen from Figure 8, Π_{AS}^{CR} is a linear function of $1/R_{EFF}$. It is worth noting that such a linear dependence is obtained also if Π_{AS}^{CR} is plotted against $1/R_C$ or $1/R_F$; i.e., this is not a particular property of R_{EFF}. The dashed line shows the same plot but for different contact angles, $\varphi_S = \alpha = 5°$. The angle of the wetting glass−water−air film in both cases is taken as $\psi_S = 0$ because the direct microscope observations show that in all experiments this angle is below 1°. As evidenced from the comparison of the solid and dashed lines in Figure 8, the variation of the contact angles does not affect significantly the magnitude of the calculated Π_{AS}^{CR} or its linear dependence on $1/R_{EFF}$.

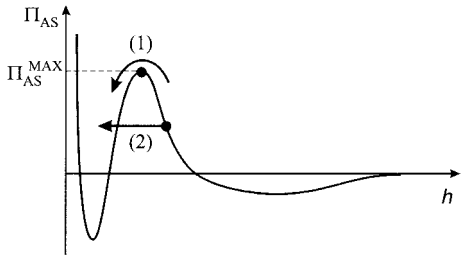

Figure 9. Schematic presentation of the disjoining pressure isotherm $\Pi_{AS}(h)$. Two ways for overcoming the barrier and possible film rupture are indicated: (1) The film surfaces are compressed against each other by a capillary pressure that drives the system to surmount the barrier Π_{MAX}—in this case the critical disjoining pressure Π_{AS}^{CR} should be equal to Π_{MAX} independently of the drop radius. (2) A local fluctuation in the film could lead to the formation of unstable spot that leads to a local film rupture.[22,57,58] In this case the film rupture may occur at a critical disjoining pressure $\Pi_{AS}^{CR} < \Pi_{MAX}$. Furthermore, Π_{AS}^{CR} could depend on the film size.[22]

The observed dependence Π_{AS}^{CR} on R_{EFF} is by no means a trivial fact. The isotherm $\Pi_{AS}(h)$ is not expected to depend on either the film size or the film curvature, because the film thickness h is much smaller than both R_{EFF} and R_F. Therefore, if the film rupture were accomplished by surmounting the maximum in the isotherm $\Pi_{AS}(h)$, then the rupture event for a given system would be expected to occur always at $\Pi_{AS}^{CR} = \Pi_{AS}^{MAX}$, independently of the drop size.

One possible explanation of the observed dependence might be related to the relatively small size of the asymmetric films. As shown previously for micrometer-sized liquid films,[53−56] the interaction force and energy across the film might be comparable in magnitude with the interaction across the meniscus region surrounding the film. If such is the case, the film destabilization will depend on the overall force of interaction between the drop and the water−air interface, including the meniscus region; i.e., Π_{AS}^{CR} should not necessarily coincide with Π_{MAX} and might depend on the film size. Another possible explanation of the experimental results is that the film rupture in our systems occurs by passing below the barrier Π_{MAX} (Figure 9), similar to the results obtained with planar foam films by Bergeron.[22] Such a possibility is offered by different theoretical models of film rupture, in which the formation of unstable spots in large liquid films by various mechanisms is considered.[22,42,57,58] However, all these models are developed for planar films and cannot be directly applied without a careful analysis of the role of film curvature in the film rupture process. For soluble oils (octane, decane, dodecane, 2BO, etc.) it was recently shown[59] that the asymmetric oil−water−air films can be

(52) Press, W. H.; Teukolsky, S. A.; Vetterling, W. T.; Flannery, B. P. *Numerical Recipes in C. The Art of Scientific Computing*; 2nd ed.; Cambridge University Press: New York, 1992.

(53) Denkov, N. D.; Petsev, D. N.; Danov, K. D. *Phys. Rev. Lett.* **1993**, *71*, 3226.

(54) Danov, K. D.; Petsev, D. N.; Denkov, N. D.; Borwankar, R. *J. Chem. Phys.* **1993**, *99*, 7179.

(55) Denkov, N. D.; Petsev, D. N.; Danov, K. D. *J. Colloid Interface Sci.* **1995**, *176*, 189.

(56) Petsev, D. N.; Denkov, N. D.; Kralchevsky, P. A. *J. Colloid Interface Sci.* **1995**, *176*, 201.

(57) Kaschiev, D.; Exerowa, D. *J. Colloid Interface Sci.* **1980**, *77*, 501.

(58) Kralchevsky, P. A.; Nikolov, A. D.; Wasan, D. T.; Ivanov, I. B. *Langmuir* **1990**, *6*, 1180.

(59) Valkovska, D. S.; Kralchevsky, P. A.; Danov, K. D.; Broze, G.; Mehreteab, A. *Langmuir* **2000**, *16*, 8892.

destabilized by a transfer of oil molecules across the film. Since the conditions in our experiments are not entirely compatible with some of the assumptions made in the respective theoretical model,[59] it is impossible to make a direct comparison of the theoretical predictions with our experimental results. Further experimental and theoretical work is intended to reveal the actual mechanism of film rupture in our systems, to modify some of the existing models or to develop a new model of this process, and to explain the observed dependence $\Pi_{AS}^{CR}(R_{EFF})$.

5. Conclusions

A systematic experimental study of the entry barriers for several oils of different chemical structure in SDDBS solutions is performed by means of the film trapping technique. First, the critical capillary pressure, P_C^{CR}, which leads to rupture of the asymmetric oil−water−air film and to drop entry at the water−air interface, is measured (for brevity, P_C^{CR} is denoted as "the entry barrier" throughout the paper). Second, the critical disjoining pressure in the moment of film rupture, Π_{AS}^{CR}, is estimated from the experimental data. The obtained results and conclusions can be summarized in the following way:

The entry barrier increases with the surfactant concentration. Close to the cmc, the increase of the entry barrier is relatively slow, whereas at about 9 mM (45 × cmc, effective volume fraction of the micelles ≈6%) the increase becomes much steeper. The latter observation implies that the micelles play a significant role in the film stabilization above a certain threshold surfactant concentration.

The presence of a spread oil layer on the surface of the solution was shown to reduce significantly the entry barrier for decane and dodecane. Remarkably, the presence of hexadecane on the solution surface (which makes a mixed adsorption layer with the SDDBS) leads to a 5-fold increase of the entry barrier with important consequences for the antifoam activity of this oil.[1] The explanation of this effect is certainly connected to the incorporation of oil molecules into the surfactant adsorption layer. However, without a more detailed picture of the mechanisms of asymmetric film rupture and drop entry, it is impossible to specify what are the properties of the mixed adsorption layer that play a major role (Gibbs elasticity, surface charge density, etc.). As far as we know, such a role of oil spreading in the antifoaming action of the oils has not been reported so far.

The entry barriers for a series of *n*-alkanes are measured in the presence of a spread oil layer. The barriers increase with the molecular mass of the alkane. Again, additional studies are needed to clarify the main factors, which govern this trend.

The calculations show that for micrometer-sized oil drops, like those in the real oil-containing antifoams, there is a big difference between the numerical values of P_C^{CR} and Π_{AS}^{CR} (unlike the case of planar films where $P_C^{CR} = \Pi_{AS}^{CR}$). The reason is that the radius of curvature of the asymmetric oil−water−air film is very small and the capillary pressure jumps across the film surfaces are very large and cannot be neglected. Therefore, one should separately consider the dependence of Π_{AS}^{CR} and P_C^{CR} on the size of the asymmetric film.

The experiments show that P_C^{CR} is a weak function of the oil drop size and of the asymmetric film radius, while Π_{AS}^{CR} scales as (film radius)$^{-1}$ for all of the studied systems. The strong dependence of Π_{AS}^{CR} on the film radius shows that the rupture of the asymmetric film does not occur simply by surmounting the barrier in the $\Pi_{AS}(h)$ curve, because the latter is expected to be independent of the film radius in the studied size range. Some possible explanations of this experimental fact are discussed.

When discussing the foam stability, P_C^{CR} is a more convenient quantity for description of the entry barriers, because its magnitude correlates with the foam height,[5,25] whereas the magnitude of Π_{AS}^{CR} does not.

Let us conclude that the film trapping technique is a powerful and versatile tool for quantifying the entry barriers of oil drops. The obtained new experimental results have posed several interesting questions concerning the general mechanism of film stability, which call for further experimental and theoretical work on this subject.

Acknowledgment. The support of this study by Colgate-Palmolive is gratefully acknowledged. The authors are indebted to Professor Ivan B. Ivanov, Professor P. A. Kralchevsky, and Dr. S. Stoyanov for the helpful discussions.

LA010601J